

Correlated electronic decay following intense near-infrared ionization of clusters

This content has been downloaded from IOPscience. Please scroll down to see the full text.

2015 J. Phys.: Conf. Ser. 635 012025

(<http://iopscience.iop.org/1742-6596/635/1/012025>)

View [the table of contents for this issue](#), or go to the [journal homepage](#) for more

Download details:

IP Address: 155.198.8.192

This content was downloaded on 26/09/2016 at 15:18

Please note that [terms and conditions apply](#).

You may also be interested in:

THE NEAR-INFRARED SPECTRUM OF VY CANIS MAJORIS

Roberta M. Humphreys

A NEAR-INFRARED CAMERA FOR LAS CAMPANAS OBSERVATORY

S. E. Persson, S. C. West, D. M. Carr et al.

FAST: A NEAR-INFRARED IMAGING FABRY-PEROT SPECTROMETER

A. Krabbe, V. Rotaciuc, J. W. V. Storey et al.

A NEAR-INFRARED STUDY OF EMISSION-LINE GALAXIES

Almudena Alonso-Herrero

H-ALPHA AND NEAR-INFRARED SPECTRA OF LATE-TYPE BE AND A-F-TYPE SHELL STARS.

A. Slettebak

A NEAR-INFRARED SURVEY OF OLD NOVAE--II. CK VULPECULAE AND V605 AQUILAE

Thomas E. Harrison

NEAR-INFRARED SURFACE PHOTOMETRY OF LATE-TYPE, EDGE-ON SPIRAL GALAXIES

David Barnaby

Correlated electronic decay following intense near-infrared ionization of clusters

Bernd Schütte^{1,4}, Mathias Arbeiter², Thomas Fennel², Ghazal Jabbari³, Alexander I. Kuleff³, Marc J. J. Vrakking¹, and Arnaud Rouzée¹

¹ Max-Born-Institut, Max-Born-Strasse 2A, 12489 Berlin, Germany

² Institut für Physik, Universität Rostock, Universitätsplatz 3, 18055 Rostock, Germany

³ Theoretische Chemie, PCI, Universität Heidelberg, Im Neuenheimer Feld 229, 69120 Heidelberg, Germany

⁴ Department of Physics, Imperial College London, SW7 2AZ London, United Kingdom

E-mail: schuette@mbi-berlin.de

Abstract. We report on a novel correlated electronic decay process following extensive Rydberg atom formation in clusters ionized by intense near-infrared fields. A peak close to the atomic ionization potential is found in the electron kinetic energy spectrum. This new contribution is attributed to an energy transfer between two electrons, where one electron decays from a Rydberg state to the ground state and transfers its excess energy to a weakly bound cluster electron in the environment that can escape from the cluster. The process is a result of nanoplasma formation and is therefore expected to be important, whenever intense laser pulses interact with nanometer-sized particles.

1. Introduction

When an excited atom or molecule is embedded in an environment such as a cluster, novel decay channels can emerge that are absent for isolated particles. Relaxation of the excited species can take place via a transfer of its excess energy to an atom or molecule in the environment that gets ionized, a process known as interatomic or intermolecular Coulombic decay (ICD) [1]. In the past, ICD has been observed following the generation of inner-shell holes in dimers [2, 3] and clusters [4] by extreme-ultraviolet (XUV) or X-ray pulses (see also review article [5]). The situation described here, i.e. the presence of an excited atom/molecule with an excitation energy that exceeds the energy needed to ionize a neighbouring atom or molecule was also at the basis of a recently proposed, alternative ICD mechanism [6]. Here energy is transferred between two excited atoms, leading to the relaxation of one excited atom to the ground state and to the simultaneous ionization of the second excited atom. As a result, an electron is emitted that has a distinct kinetic energy [7]. This process could be experimentally confirmed in Ne clusters [8, 9] and in He nanodroplets [10, 11] following resonant excitation using intense XUV radiation from free-electron lasers.

The interaction of clusters with near-infrared (NIR) laser pulses is fundamentally different from the XUV and X-ray regimes. Excitation or ionization of atoms in the cluster can only occur at sufficiently high NIR intensities that are required for triggering multiphoton processes. Once the cluster gets ionized, highly nonlinear dynamics have been observed that can lead to



very high ion charge states [12], extremely high ion kinetic energies up to 1 MeV [13] and efficient X-ray generation [14]. Due to the build-up of the cluster potential after the escape of the first electrons (referred to as outer-ionized electrons), a large fraction of the so-called inner-ionized electrons remain trapped within the cluster, and a nanoplasma is formed [15]. The electrons are accelerated in the NIR laser field and can trigger efficient impact ionization leading to an avalanche of ionization processes. In the past, the measured electron kinetic energy spectra from clusters typically exhibited continuous contributions with no bound-state signatures visible [16, 17]. Therefore, electron emission from clusters interacting with intense NIR laser pulses is often understood as a combination of direct outer ionization processes and evaporation of electrons from an equilibrated nanoplasma that exhibits a delayed emission profile [15].

In the current study, we present novel experimental results on the ionization of Ar clusters with intense NIR laser pulses. We report on the observation of a peak in the electron kinetic energy spectrum just below the ionization potential IP of atomic argon ($IP = 15.76$ eV). Our experimental and theoretical investigations suggest that this so far unobserved contribution is due to correlated electronic decay (CED), where energy is transferred between two electrons bound in a cluster. The process takes place in two steps: In the first step, extensive Rydberg atom formation via electron-ion recombination takes place in the nanoplasma [18, 19, 20]. In the second step, the excess energy from the de-excitation of an excited atom initially in a Rydberg state is transferred to a nearby, weakly bound electron (either another Rydberg electron or a quasifree electron that is bound by the cluster potential). As a result, one of the two electrons can escape from the cluster with an initial kinetic energy close to IP . We have time-resolved CED by depopulating the excited state levels with a time-delayed weak NIR probe pulse, giving a CED time of 87 ps. CED is of universal nature, as it is a result of nanoplasma formation. It is therefore not restricted to a certain wavelength regime or system and was observed in all clusters that we investigated.

2. Experimental setup

For the experiments, we use a Ti:sapphire laser at a central wavelength of 790 nm and a repetition rate of 50 Hz. The laser delivers pulses with a duration of 32 fs and a maximum energy of 32 mJ [21]. The pulses are split into a pump and probe beam, for which an interferometric setup is employed making use of a motorized delay stage. In our setup two separate grating compressors are used to adjust the pulse durations of pump and probe pulses independently. The pulse energies of the pump and probe beams can be adjusted with irises and neutral density filters. Both beams are recombined by a mirror with a central 6 mm diameter hole that transmits the pump beam, while the outer part of the probe beam is reflected by the mirror. The beams propagate collinearly and are focused by a spherical mirror with a focal length of 75 mm into a cluster jet generated by a pulsed piezoelectric valve. The average cluster size is controlled by varying the backing pressure and is estimated according to the Hagena scaling law [22]. A velocity-map imaging spectrometer is used to record electron momentum distributions [23]. The generated electrons are accelerated by a static electric field and are detected by a microchannel plate / phosphor screen assembly in combination with a CCD camera. In order to obtain the electron kinetic energy spectra from the measured momentum distributions, we apply a standard Abel inversion method [24] and integrate over all emission angles.

3. Results

3.1. Spectral signatures of correlated electronic decay

We investigated the ionization of medium-sized rare-gas and molecular clusters by NIR pulses with average intensities around 1×10^{14} W/cm². As an example, an electron kinetic energy spectrum following NIR ($I = 1.2 \times 10^{14}$ W/cm²) ionization of Ar clusters with an average size of $\langle N \rangle = 200$ atoms is shown in Fig. 1 using a logarithmic scale. The gray-shaded area represents an

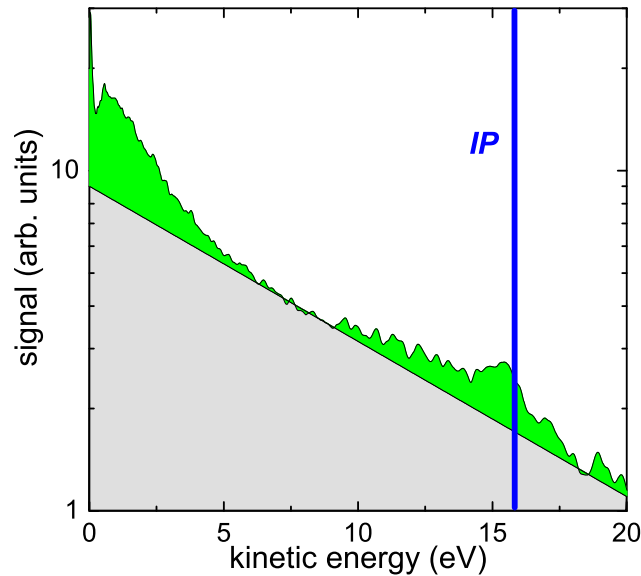


Figure 1. Electron kinetic energy spectrum recorded from Ar clusters with an average size of $\langle N \rangle = 200$ atoms following ionization by NIR pulses with an intensity of 1.2×10^{14} W/cm² and a pulse duration of 32 fs. The peak below the ionization potential of Ar at 15.76 eV (marked by the blue line) is attributed to correlated electronic decay, whereas the gray area represents thermal electron emission from the nanoplasma.

exponential electron distribution that is characteristic for thermal electron emission. In addition, a peak is visible close to the *IP* of atomic Ar, which is a clear indication of an electron emission process involving atomic bound states. This electron emission was found to be isotropic [25], indicating that no information of the initial NIR pump laser polarization is preserved. The electron emission is attributed to a correlated electronic decay, where energy is transferred from a localized electron in an atomic Rydberg state to a second nearby electron. For example, our results are compatible with an ICD process between two highly excited Rydberg atoms, where one electron relaxes to the ground state, and the excess energy is transferred to a Rydberg electron in the second atom that can escape from the cluster. The latter electron acquires an initial kinetic energy of $\approx IP$, in accordance with the experimentally observed peak. The second electron may also be delocalized in the nanoplasma instead of being bound to a specific atom [25]. In addition to the peak at 15.5 eV, electron signal exceeding the thermal emission is found below 5 eV, between 8 and 15 eV and at kinetic energies between 16 and 20 eV (Fig. 1). The tail towards lower kinetic energies between 8 and 15 eV can to some extent be explained by lower excited states that are involved in the CED process and by electrons emitted via CED processes that take place at the early stage of the cluster expansion. These electrons interact with the charged cluster environment, leading to a decrease of their kinetic energies. We note that electrons may also be emitted via autoionization of doubly-excited atoms [26], which can contribute to the observed electron signal exceeding the thermal electron distribution in Fig. 1. The electron contribution between 16 and 20 eV on top of the exponential curve may be due to such autoionizing processes of doubly-excited atoms. It is furthermore possible that an Ar⁺* ion decays to the ionic ground state by transferring its excess energy to a quasifree electron or to an excited atom / ion in the environment that gets ionized. This can explain the emission of electrons with kinetic energies above the first ionization potential.

This new contribution was observed in all systems that we investigated, including Kr, Xe, O₂

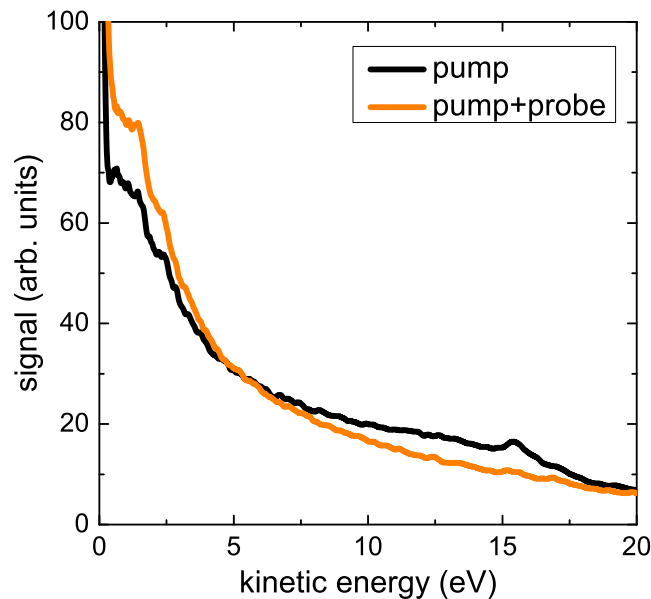


Figure 2. Electron kinetic energy spectrum from Ar clusters with an average size of $\langle N \rangle = 1000$ atoms ionized by NIR pulses with an intensity of 1×10^{14} W/cm² and a pulse duration of 32 fs (black curve). The signal attributed to CED is quenched, when an additional NIR probe pulse with an intensity of 2×10^{13} W/cm² and a pulse duration of 1 ps is used that is delayed by 4 ps with respect to the pump pulse (orange curve).

and CH₄ clusters. However, a clear peak structure in the electron spectrum was only identified in a narrow range of intensities. In Ar clusters with an average size of $\langle N \rangle = 1000$ atoms, we did not observe a peak when the NIR intensity was only 5×10^{13} W/cm², which we attributed to the low degree of inner ionization of the cluster and the correspondingly low density of Rydberg atoms formed via electron-ion recombination [25]. At an intensity of 1×10^{14} W/cm², the peak was most clearly visible and was detected at a kinetic energy close to *IP*. When the intensity was further increased to 2×10^{14} W/cm², the peak was still visible, but it was clearly broadened and shifted towards lower kinetic energies [25]. At higher intensities, the cluster becomes more highly charged and the enhanced interaction of CED electrons with the cluster environment leads to the observed broadening and energy downshift. Increasing the size of the cluster leads as well to a shift of the peak towards lower kinetic energies [25].

3.2. Temporal investigation of correlated electronic decay

In order to estimate the decay time of the CED emission, a second NIR probe pulse with an intensity of 2×10^{13} W/cm² and a pulse duration of 1 ps was used to efficiently depopulate the Rydberg states before CED can take place. The probe pulse intensity was chosen to avoid ionization of the clusters by the probe pulse only. In Fig. 2, the electron kinetic energy spectrum following ionization of Ar clusters with an average size of $\langle N \rangle = 1000$ atoms is shown without (black curve) and with the probe pulse at a time delay of 4 ps (orange curve).

With the probe pulse, the electron signal significantly increases at kinetic energies below 4 eV, whereas a decrease of the signal for electron kinetic energies between 7 to 17 eV is observed. The reionization of Rydberg atoms that are formed by electron-ion recombination processes by absorption of one or more NIR probe photons is responsible for the increase of the signal at low kinetic energies (cf. Refs. [19, 20]) and prevents at the same time the CED process to take place. As a result, the peak close to the *IP* almost disappears in Fig. 2. By varying the time

delay between the pump and probe pulses, we were able to extract the timescale for the CED process under our experimental conditions, for which we found a value of 87 ps.

In comparison, a recent time-resolved ICD investigation on Ne dimers ionized by XUV pulses reported a much shorter decay time of 150 fs [27]. We have performed an *ab initio* calculation [28] of the decay rate of a dimer formed by two atoms in their lowest excited states. For the lowest four states of the Ar*(4s)Ar*(4s) dimer at the equilibrium distance (3.8 Å), we find decay times between 100 and 550 fs, with an average value of 200 fs. In our experiment, no peak is observed at 7.3 eV, which would correspond to the expected electron kinetic energy after ICD of the Ar*(4s)Ar*(4s) dimer. This is explained by the fact that the cluster is still dense after 200 fs, and the emitted electrons exchange energy with their surroundings (see below). In order to rationalize the much longer decay times measured in our experiment, we have further estimated the decay times between atoms in higher excited states according to the virtual-photon model of ICD reported in Ref. [28]. In this model, ICD is described by the emission of a virtual photon from the de-excitation of an excited atom. This virtual photon is absorbed by the second excited atom that gets ionized. The corresponding decay width from this model can be estimated according to [6] by

$$\Gamma(R) = \frac{3cf\sigma}{\pi\omega^2} \frac{1}{R^6}, \quad (1)$$

with c being the speed of light, f being the oscillator strength of the considered transition in the first excited atom, and σ the ionization cross section of the second excited atom. ω is the energy of the virtual photon, and R is the distance between the two atoms. As an example, we consider the decay of an Ar*(7s)Ar*(7s) dimer. For $n = 7$, the cross section and the oscillator strength are both reduced by a factor of about 10 when compared to $n = 4$ [29, 30]. In addition, ω^2 is increased by a factor of 1.7. This model shows that dimers consisting of two atoms in higher excited states may have decay times in the order of tens of ps, which is compatible with the experimental observation. As already discussed, other processes than ICD such as mechanisms involving delocalized electrons or autoionization of doubly-excited atoms may play a role as well.

CED electrons emitted on faster time scales exchange energy with the charged cluster environment, as we have demonstrated by molecular dynamics calculations [25, 31]. Electrons originating from CED processes on a fs time scale are likely to remain trapped within the cluster due to the deep cluster potential at the early stages of the cluster expansion. Electrons from CED processes emitted on a few ps time scale may escape from the cluster, but their final kinetic energies are affected by the strong cluster potential. Only electrons that are generated at times when the cluster has already significantly expanded, can contribute to the observed peak close to the ionization potential. In general we can expect that CED processes are most efficient at higher densities of excited atoms, ions and electrons, i.e. at earlier stages during the cluster expansion on a fs time scale. Novel experimental schemes that make it possible to observe and investigate CED processes that take place at the early stages of the cluster expansion are therefore highly desirable in order to better understand nanoplasma dynamics.

4. Summary and outlook

In summary, we have reported on a previously unobserved correlated electronic decay process following the ionization of clusters by intense NIR pulses. A clear peak structure is visible in the electron kinetic energy spectrum, demonstrating that relaxation processes involving energy exchange between weakly bound/quasifree electrons play an important role in expanding clusters. We could estimate a decay time of 87 ps for CED processes following ionization of Ar clusters by an NIR laser field, which is consistent with the virtual photon model of ICD for a dimer composed of atoms in high-lying Rydberg states. We can expect as well that faster CED processes involving lower excited states take place in nanoplasmas at the early stage of the cluster expansion. However, molecular dynamics calculations show that electrons emitted on a

fs to few ps time scale heavily exchange energy with the charged cluster environment, making their observation very challenging.

In the future, extensive experimental and theoretical investigations are needed in order to evaluate the overall significance of CED in nanoplasmas generated from different systems and with laser pulses at different wavelengths. As an example, CED may also take place during and after the interaction of intense X-ray pulses with biomolecules, which is of high interest for single-shot X-ray diffraction imaging experiments. The possibility to carry out experiments on these nanoplasma dynamics using table-top setups offers unprecedented opportunities in the future for the investigation of electron-correlation-driven energy transfer processes in nanometer-sized systems.

5. Acknowledgments

We would like to thank V. Averbukh, K. Gokhberg and L.S. Cederbaum for fruitful discussions. B.S. acknowledges financial support by the DFG via a research fellowship. T.F. and M.A. acknowledge computer time provided by the North-German Supercomputing Alliance (HLRN, project no. mvp00004), and financial support by the DFG through the SFB 652. A.I.K. and G.J. thank K. Gokhberg for the help with computations. A.I.K. acknowledges the financial support by the ERC AdG No. 227597, and G.J. thanks IMPRS-QD for financial support.

References

- [1] Cederbaum L S, Zobeley J and Tarantelli F 1997 *Phys. Rev. Lett.* **79** 4778
- [2] Jahnke T *et al.* 2004 *Phys. Rev. Lett.* **93** 163401
- [3] Trinter F *et al.* 2014 *Nature* **505** 664
- [4] Marburger S, Kugeler O, Hergenhanhn U and Möller T 2003 *Phys. Rev. Lett.* **90** 203401
- [5] Jahnke T 2015 *J. Phys. B* **48** 082001
- [6] Kuleff A I, Gokhberg K, Kopelke S and Cederbaum L S 2010 *Phys. Rev. Lett.* **105** 043004
- [7] Demekhin Ph V, Gokhberg K, Jabbari G, Kopelke S, Kuleff A I and Cederbaum L S 2013 *J. Phys. B* **46** 021001
- [8] Nagaya K *et al.* 2013 *J. Phys. B* **46** 164023
- [9] Yase S *et al.* 2013 *Phys. Rev. A* **88** 043203
- [10] LaForge A C *et al.* 2014 *Sci. Rep.* **4** 3621
- [11] Ovcharenko Y *et al.* 2014 *Phys. Rev. Lett.* **112** 073401
- [12] Snyder E M, Buzzza S A and Castleman Jr S A 1996 *Phys. Rev. Lett.* **77** 3347
- [13] Ditmire T, Tisch J W G, Springate E, Mason M B, Hay N, Smith R A, Marangos J P and Hutchinson M H R 1997 *Nature* **386** 54
- [14] Ditmire T, Donnelly T, Falcone R W and Perry M D 1995 *Phys. Rev. Lett.* **75** 3122
- [15] Ditmire T, Donnelly T, Rubenchik, A M, Falcone R W and Perry M D 1995 *Phys. Rev. A* **53** 3379
- [16] Shao Y L, Ditmire T, Tisch J W G, Springate E, Marangos J P and Hutchinson M H R 1996 *Phys. Rev. Lett.* **77** 3343
- [17] Springate E, Aseyev, S A, Zamith S and Vrakking M J J 2003 *Phys. Rev. A* **68** 053201
- [18] Schütte B, Arbeiter M, Fennel T, Vrakking M J J and Rouzée A 2014 *Phys. Rev. Lett.* **112** 073003
- [19] Schütte B, Campi F, Arbeiter M, Fennel T, Vrakking M J J and Rouzée A 2014 *Phys. Rev. Lett.* **112** 253401
- [20] Schütte B, Oelze T, Krikuonva M, Arbeiter M, Fennel T, Vrakking M J J and Rouzée A 2015 *New J. Phys.* **17** 033043
- [21] Gademann G, Plé F, Paul P-M and Vrakking M J J 2011 *Opt. Express* **19** 24922
- [22] Hagena O F and Obert W 1972 *J. Chem. Phys.* **56** 1793
- [23] Eppink A T J B and Parker D H 1997 *Rev. Sci. Inst.* **68** 3477
- [24] Vrakking M J J 2001 *Rev. Sci. Inst.* **72** 4084
- [25] Schütte B *et al.* 2015 *Nat. Commun.* **6** 8596
- [26] Schütte B, Lahl J, Oelze T, Krikuonva M, Vrakking M J J and Rouzée A 2014 *Phys. Rev. Lett.* **114** 123002
- [27] Schnorr K *et al.* 2013 *Phys. Rev. Lett.* **111** 093402
- [28] Averbukh V and Cederbaum L S 2005 *J. Chem. Phys.* **123** 204107
- [29] Chang T N and Kim Y S 1982 *Phys. Rev. A* **26** 2728
- [30] Zatsarinny O and Bartschat K 2006 *J. Phys. B* **39** 2145
- [31] Arbeiter M, Peltz C and Fennel T 2014 *Phys. Rev. A* **89** 043428